Organic Electronics 111 (2022) 106665

Contents lists available at ScienceDirect

Organic Electronics

journal homepage: www.elsevier.com/locate/orgel

Effects of PCBM loading on high sensitive P3HT based vertical bulk resistive X-ray detector

Yalçın Kalkan [a], Sadullah Öztürk [b], Arif Kösemen [b,c,*]

[a] Department of Physics, Bolu Abant İzzet Baysal University, Bolu, Turkey
[b] Institute of Nanotechnology and Biotechnology, Istanbul University-Cerrahpasa, Istanbul, Turkey
[c] Department of Detector and Sensor Technologies, Muş Alparslan University, Muş, Turkey

ARTICLE INFO

Keywords:
X-ray detection
Dosimetry
Organic X-ray detector
Graphite electrode
P3HT:PCBM

ABSTRACT

Recently, semiconductive polymeric materials have attracted attention as an active layer for detecting ionizing radiation because of their excellent properties such as flexibility, easy production, solution processability and low-cost production. This paper presents X-ray detection properties of Poly(3-hexylthiophene) (P3HT):Phenyl C61 butyric acid methyl ester (PCBM) blend structure with different PCBM loading ratios. P3HT:PCBM mixing ratio was changed from 1:0 to 1:2. Top contact of the pure and blend structured device were produced by using a solution based graphite ink. Devices were constructed with vertical bulk resistive architecture within an ohmic electrode structure as ITO/PEDOT:PSS/P3HT:PCBM/Graphite configuration. Graphite electrode was coated on the active layer with the spray coating method. All devices exhibited ohmic current-voltage (I–V) characteristics. The blend structured devices exhibited stable saw-tooth type behaviour in photocurrent responses against the on and off states of X-rays. Saw-tooth type responses could be evaluated as major evidence for a potential usage of organic electronic device technology direct radiation detectors. Although the best sensitivity value to X-ray was obtained with the blend structure with equal ratio, it was observed that the rise and decay times were shortened with the increase in the amount of PCBM in the blend structure from.

1. Introduction

Ionizing radiation detectors, which are constantly evolving to meet different needs for various usage purposes, are used in many areas such as medical physics applications [1], security and defence [2], particle physics [3], and nuclear physics applications [4]. Radiation can be detected in two ways as direct and indirect methods. Indirect methods rely on a secondary transmission, such as modulation/quenching of optical properties or luminescence along with a phosphor screen is known as indirect radiation detection methods [5]. Additionally, indirect detectors have a more complex and less efficient structure, especially in medical dosimetry applications [6]. Direct radiation detection method based on photocurrent induction, which can be quantitatively correlated with the radiation dose exposed to a radiation-sensitive material, is highly suitable for practical applications. Direct detectors compete with scintillation based indirect detectors because of their high sensitivity, low signal noise and better spatial resolution [6].

Research on alternative materials for ionizing radiation detection is increasing rapidly [7]. Solid-state detector materials (such as silicon (Si), cadmium zinc telluride (CdZnTe), mercury iodide (HgI_2), etc.) can directly detect radiation used classically for a long time, but they have serious limitations in large-area pixel detector applications [8–11]. Inorganic-based X-ray detectors have negative parameters such as large-scale production, high cost and fragile property. In particular, flexible device applications based on inorganic materials are difficult, and although flexibility can be achieved only using a thin inorganic layer, which cause to reduce the active layer thickness and thus its X-ray absorbency [12].

Recently, as an alternative to inorganic materials semiconductive organic materials have started to attract attention and interest duo to their impressive chemical and physical properties. Research and development studies on organic electronic devices span a wide range from sensors to light emitting diodes (LEDs) [13–18]. Moreover, potential and volume in commercial usage of organic materials in organic electronic device technology have been developed by replacing inorganic based counterparts particularly display and photovoltaic technologies. Organic electronic devices can be fabricated by various low-cost and solution-processable techniques [19].

* Corresponding author. Institute of Nanotechnology and Biotechnology, Istanbul University-Cerrahpasa, Istanbul, Turkey.
E-mail address: arif.kosemen@iuc.ed.tr (A. Kösemen).

https://doi.org/10.1016/j.orgel.2022.106665
Received 1 July 2022; Received in revised form 7 October 2022; Accepted 9 October 2022
Available online 12 October 2022
1566-1199/© 2022 Published by Elsevier B.V.

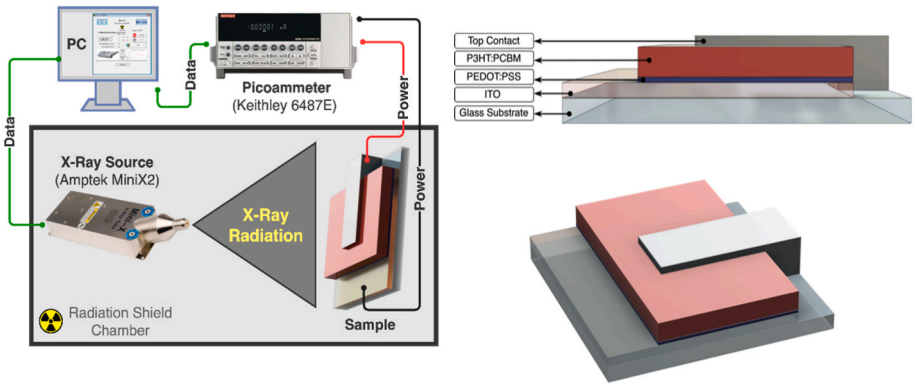

Fig. 1. Schematically illustration of the X-ray Measurement Set-up.

Furthermore, semiconductor based organic materials has a potential usage in nuclear medicine techniques thanks to their tissue-equivalent and non-toxic harmless ingredients in terms of chemical structures [20]. In recent, organic electronic device applications have been broadened to X-Ray radiation detectors which can be used in medical diagnostics, cancer therapy, material inspection and scientific research [21]. Boroumand et al. reported the first direct X-ray detection of X-ray induced photocurrents in thick films of conjugated polymers using poly [1-methoxy-4-(2-ethylhexyloxy)-phenylenevinylene] (MEH-PPV) and poly (9,9-dioctylfluorenyl-2,7-diyl) (PFO) [22]. Intaniwet et al. compared the performance of polymer-based X-ray detectors obtained using metal electrodes such as Al, Au, Ni and Pd [6,23] and presented the first-ever measured charge transport properties of PTAA: TIPS-pentacene blends using a time-of-flight (TOF) photocurrent measurement technique [24]. Han et al. demonstrated a flexible polymer-based X-ray detector and improved X-ray detection sensitivity using single-walled carbon nanotubes (SWNTs) [25]. Griffith et al. studied the recent applications of organic semiconductor materials in radiation detection and reported on various materials and manufacturing innovations aimed at creating, maintaining, and characterizing the nanoscale structure of organic semiconductor materials for radiation detection during large-area print production [26]. Nanayakkara et al. reported a study on obtaining ultra-low dark currents under high electric fields in the hole transport layer [21]. Ciavatti et al. developed an alternative approach to increase the radiation capture cross section that takes advantage of the tunability of organic materials by incorporating high Z atoms into the basic molecular structure [27]. Hupman et al. developed a method to measure foreign signals produced by thin-film radiation-sensing diodes, and with this method, they made measurements in radiation fields using a P3HT/PCBM bulk heterojunction (BHJ) photodiode [28]. Valitova et al. have developed an application for the use of Poly(3-hexylthiophene-2,5-diyl) (P3HT)-based organic diodes as potential radiation dosimeters by describing the mechanism of radiation-induced photocurrent under various conditions [20].

Chemical and electronic stability, high carrier mobility, low leakage currents (dark current), and high current sensitivity during radiation exposure are critical parameters for charge-based radiation detection by using polymeric diodes. In addition, the use of polymer-based diodes for charge-based radiation detection is useful by having a large thickness to increase the “capture volume” of the active material [29].

This work is focused on the direct detection of X-ray radiation with conductive polymer materials. P3HT:PCBM (poly(3-hexylthiophene): phenyl-C61-butyric acid methyl ester) system was used as an active layer and investigated how to effect PCBM concentration on X-ray detection sensitivity. Our devices were fabricated as ITO/PEDOT:PSS/P3HT:PCBM/Graphite electrode structures. Graphite electrode was coated on the active layer with the spray coating method.

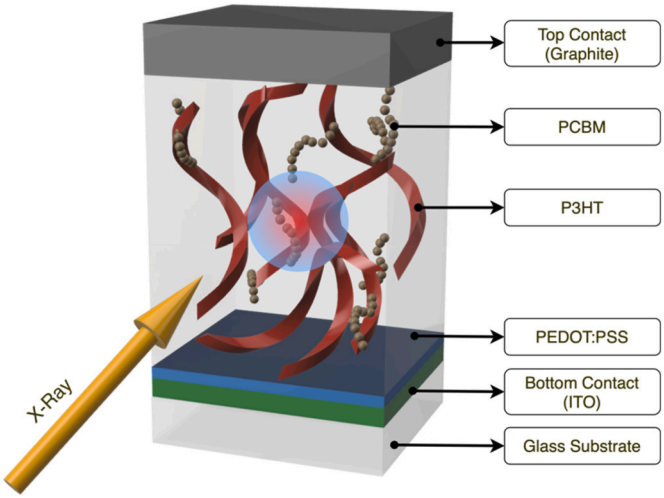

Fig. 2. Schematic structure of the devices.

2. Experimental section

Poly(3-hexylthiophene-2,5-diyl) (P3HT), C61-butyric acid methyl ester (PCBM) were purchased from Aldrich and used without any further purification. Graphite solution (Graphite 33) was used to coat top electrode and purchased from purchased from Kontakt Chemie. P3HT (30 mg) and PCBM (0, 15, 30 and 60 mg) were firstly mixed in chloroform (1 ml) with different concertation ((1:0), (1:0.5), (1:1), (1:2)) (wt/wt) ratio at 50 °C for a night.

In order to prepare the devices first of all ITO (Indium Tin Oxide) coated glass substrates subject to a standard cleaning process with acetone, ethanol, and distilled water in the ultrasonic bath for 15 min to each cleaning agent. Poly(3,4-ethylenedioxythiophene) (PEDOT:PSS) layer was coated on cleaned ITO coated glass substrate with spin coater at 4000 rpm as a charge transport layer. P3HT:PCBM solution was drop cast on PEDOT:PSS layer, dried in atmospheric conditions and annealed at 120 °C for 30 min to eliminate residual solvents. The thickness of the P3HT:PCBM layers was measured approximately as 20 μm by using cross-sectional view of SEM images.

Graphite electrode was coated on P3HT:PCBM layer with the spray coating method and annealed at 90 °C for 60 min and the thickness of the Graphite electrode was obtained from SEM images as approximately 3 μm.

All the measurements were carried out in ambient conditions at room temperature using an active area of 0.15 cm^2. Electrical measurements were achieved with a Keithley 6487E Picoammeter. Radiation measurement studies were conducted at room temperature with an Amptek Mini X2 X-ray tube (focal spot size approximately 2 mm), X-rays

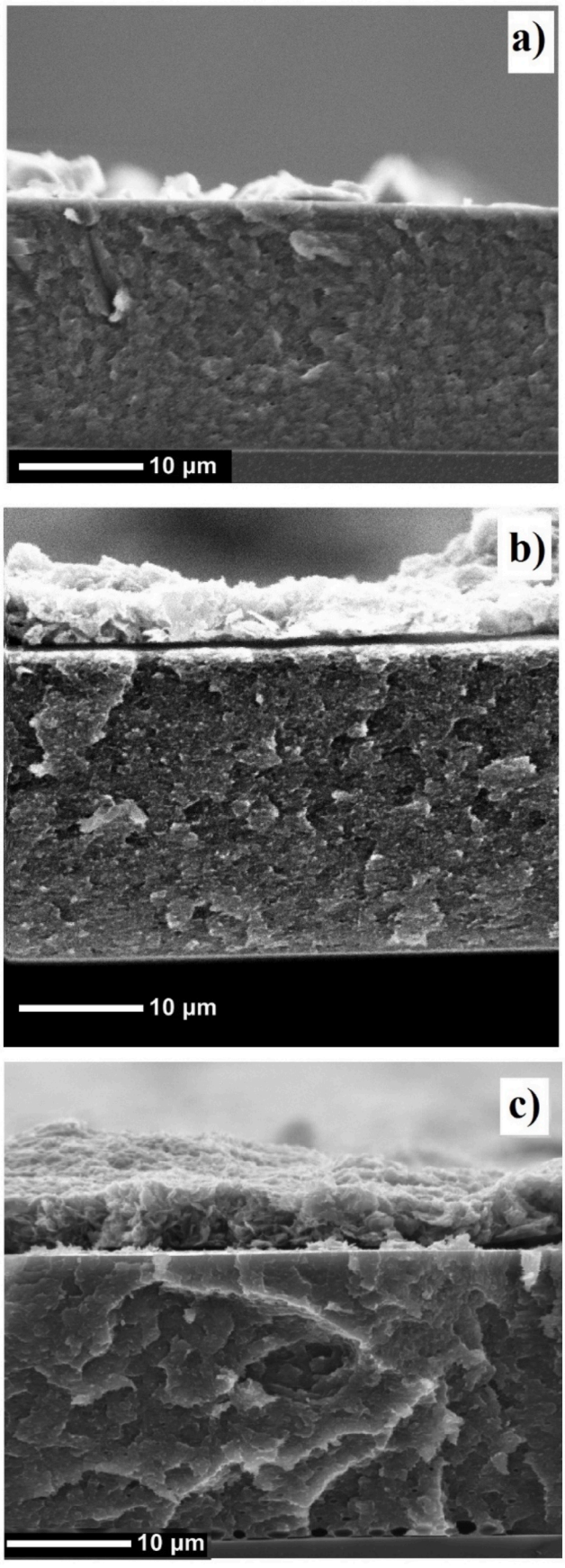

Fig. 3. SEM images of the PCBM loaded P3HT for different concentration of P3HT:PCBM mixtures a) 1:0.5 b) 1:1, c) 1:2.

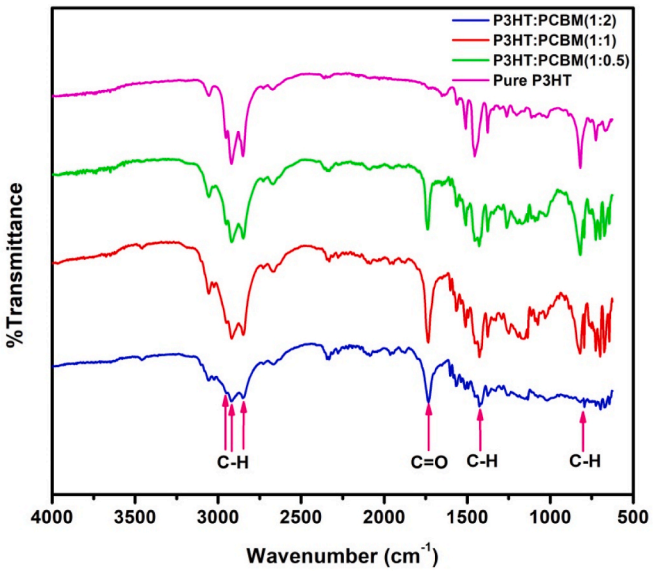

Fig. 4. FTIR spectrum of the polymer materials.

produced from a gold target along with a continuous spectrum extending to the electron energy corresponding to the applied tube bias. To adjust the dose rate, tube voltage was altered from 10 kV to 50 kV. Current versus voltage (I–V) characterization studies were carried out by using a Fytronix 9712 source-meter at room temperature and ambient conditions. Schematically illustration of measurement setup and device structure (in isometric and cross-sectional view) was given in Fig. 1.

3. Results and discussions

The detector devices were constructed of a bulk resistive structure where pure P3HT and Bulk Hetero Junction (BHJ) P3HT:PCBM mixture is sandwiched between Indium Tin oxide (ITO) and Graphite electrodes (Fig. 2).

Cross-sectional SEM images of the fabricated devices SEM images were presented in Fig. 3 and used for analyzing either thickness of organic structures and graphite electrodes and, PCBM loading concentration. It is clearly seen that from Fig. 3 PCBM distribution is homogeneous for different concentrations. The thicknesses of the active layers was measured from the SEM images as ~19.3 μm for 1:05, ~24 μm for

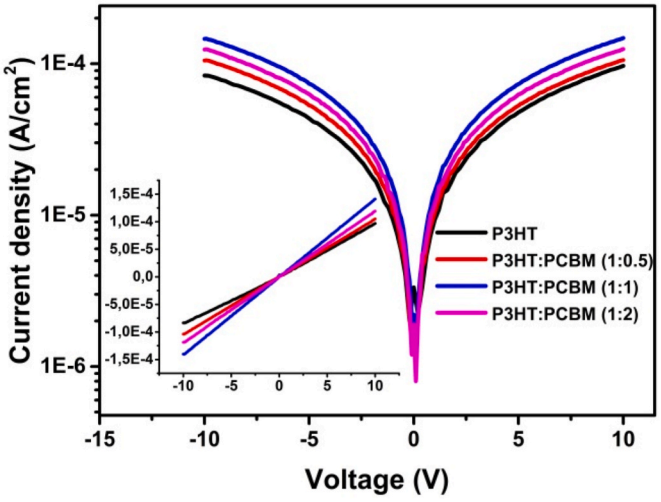

Fig. 5. Current-Voltage Characteristic of the fabricated devices under dark conditions.

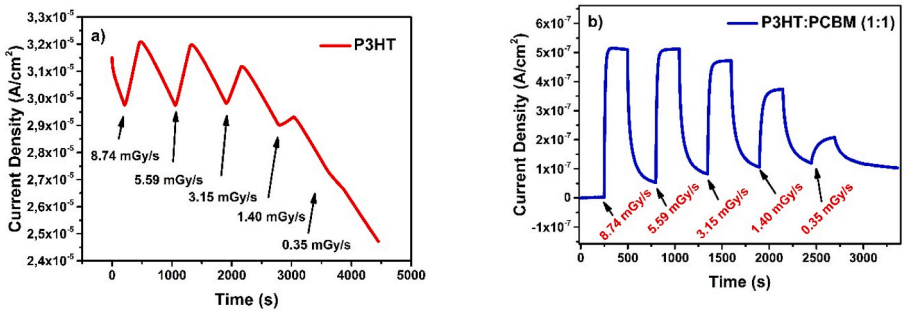

Fig. 6. X-ray photocurrent responses of fabricated (a) pure P3HT and (b) P3HT:PCBM bland structure devices.

1:1, and ~24.6 μm for 1:2 P3HT:PCBM mixtures.

The chemical structures of X-ray sensitive polymer based devices as pure P3HT and P3HT:PCBM (1:1) were analyzed to investigate bonding interactions using Fourier Transformed Infrared spectroscopy technique in transmission mode. FTIR spectrum of the polymer materials were depicted in Fig. 4. Characteristic peaks of the P3HT were observed at 2952, 2919 and 2851 cm^{-1} attributed to C–H vibrations in the aliphatic chain of hexyl groups. The bending vibrations of C–H bond used for specifying of the thiophene ring was observed at 1456 cm^{-1} for pure P3HT and P3HT:PCBM (1:1) blend structures. Moreover, bending of aromatic C–H was observed at 819 cm^{-1} [30]. While no stretching vibration C═O for pure P3HT, intense peaks were observed for PCBM loaded P3HT blend polymer structures at 1732 cm^{-1} and it is characteristic for fullerene. Furthermore, presence of this peak indicates that a covalent bond is formed between P3HT and PCBM [31].

P3HT and PCBM mixtures were chosen as the active layer because of their well-known and relatively stability. A soluble graphite electrode was used as a top electrode, which can allow large area fabrication and easy production techniques. It is clearly seen that from Fig. 5, all devices exhibited ohmic behavior with this electrode system. Current versus to voltage (I–V) characteristics of the devices were carried out between −10 and + 10 V. The linear I–V characteristics of the devices indicate that the contacts between the active layer and contact electrodes (ITO as bottom contact and Graphite as top contact) were ohmic. It is aimed that with this electrode configuration to fabricate vertically resistive devices.

Principally, pure P3HT and P3HT:PCBM (1:1) active layer devices were analyzed with a dynamic measurement system at 10V bias and under dark and X-ray on conditions. The X-ray photocurrent responses of the two fabricated devices based on pure P3HT and blend structured P3HT:PCBM (1:1) exposed under different X-ray radiation dose rates were given in Fig. 6. Different exposure and aging in the dark condition time was applied according to X-ray response characteristics of the fabricated device. X-ray exposure (300s) and aging in dark conditions (600s) times are for pure P3HT and exposure (150s) and aging in dark conditions (300s) times are for P3HT:PCBM devices. X-ray radiation dose rates were stated in each graph. The arrow for each dose rate also indicates the time when X-ray was initiated to be applied to the devices. According to Fig. 6, applied X-ray dose rate decreased from 8.74 mGy s^{-1} to 0.35 mGy s^{-1}. The current density of the pure P3HT based device increased when exposed to the X-ray. The change in the current density of the pure P3HT is nearly same for 8.74 mGy s^{-1} and 5.59 mGy s^{-1} dose rates but change in the current density is decreased by lowering dose rates. It is clearly seen in Fig. 6 (a) that when the pure P3HT-based device is exposed to X-ray with the lowest dose rate, the change in current density is incomparably lower than other dose rates. Moreover, pure P3HT based device was exposed to the X-ray, current density started to increase, but never reached to a steady state value in 300s for any dose rates. On the other hand, it could be observed that in Fig. 6 (b), current density of the P3HT:PCBM(1:1) device increased with the exposure of the X-ray and current were decreased down when X-ray was off. Furthermore, The change in current density decreased due to the decrease in the applied X-ray dose rate. Moreover, when P3HT:PCBM (1:1) devices were exposed to X-ray, current density reached to the steady state value approximately in 40s. When an X-ray was off, current density decreased and reached to a significant baseline stage approximately 50s. The current density characteristic of the blend structured device was saw-tooth shaped. The saw-tooth structure of the current density by applying X-ray dose rates over time shows the potential use of the X-ray detection with organic semiconducting electronic devices.

Semiconducting organic polymers, unlike inorganic structures, have discrete energy levels due to the lack of crystal structure, so the difference between discrete energy levels of organic polymers is large. Due to the large band gap (~2 eV), the population of free charge carriers produced by thermal excitation is low. So, this makes it easier to monitor the change in the number of free charge carriers in the semiconductor material, especially by the excitation of organic semiconductor polymers with electromagnetic waves, and this is called as photocurrent [32]. Photocurrent is formed by the separation of excitons composed of electron and hole pairs in the semiconductor and separated charges move to the opposite electrodes. Only the change in the current density

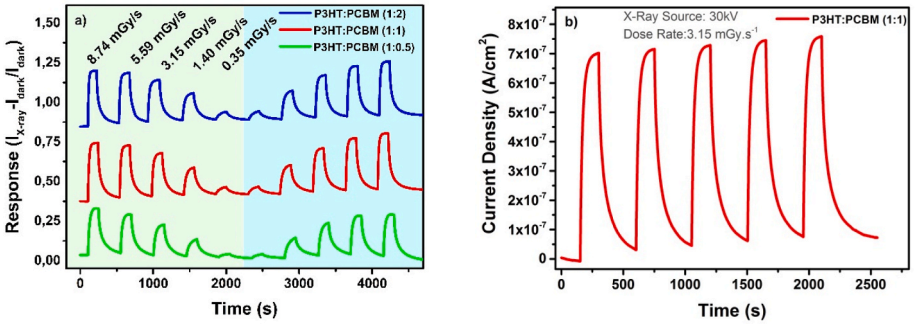

Fig. 7. Photo current responses of the P3HT blended with various PCBM concentrations under different X-ray radiation dose rates (a). Photo-current versus time plot of P3HT:PCBM (1:1) device under same dose rate radiation as 3.15 mGy s^{-1} and exposed to for five times.

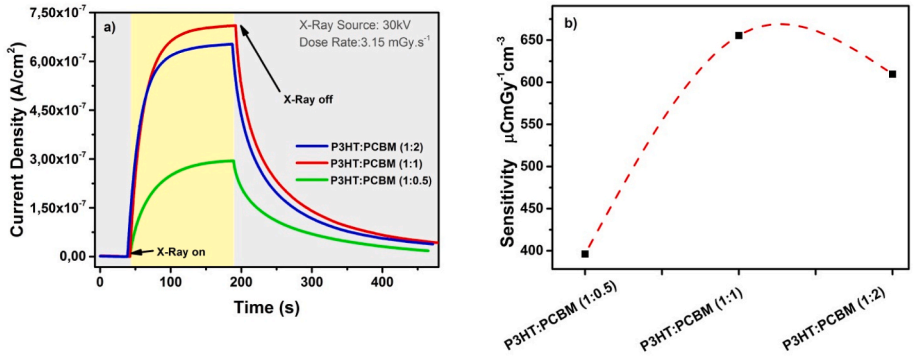

Fig. 8. X-ray photocurrent densities (a) and sensitivity (b) for devices with different PCBM loadings from PCBM-0.5 to PCBM-2.

because of the photocurrent of the P3HT-based device constantly increases, while the photocurrent-based current density of the P3HT:PCBM (1:1) based device reaches a stable level after a while. The main factor in reaching the stable level of the current density of the P3HT:PCBM (1:1) device is the rapid dissociation of the electron-hole pairs formed by X-ray exposure. In order to dissociate excitons, a high electric field has to be applied to the devices, but this is not properly practical. Therefore, producing of dispersed p-n junctions centers or regions in the semiconducting materials is so useful. As a result of the combination of p-type semiconductor P3HT and n-type semiconductor PCBM as a blend structure, donor-acceptor centers are formed in the entire organic electronic device, enabling rapid separation of excitons and as a result, a stable current density level is observed. In the pure P3HT-based device only, although the formation of excitons continues continuously with X-ray, the rate of increase in the current density was quite slow due to the absence of acceptor-donor centers for separating excitons, and a stable level was reached [32].

In order to investigate the PCBM loading ratio effect on the X-ray detection sensitivity amount of PCBM in the active layer was changed. Fig. 7 (a) shows the responses of the P3HT blended with various PCBM concentrations under different X-ray radiation dose rates. One of main aims of this works understood of the device characteristics and repeatability of the fabricated devices depends on the dose rate, continuous measurements and to understand whether the destructive effects of radiation on the device performance. X-ray radiation measurements were realized by decreasing the dose rate (light green region in Fig. 7(a)) and then increasing the dose rate (light blue region in Fig. 7(a)). In decreasing the radiation dose rate fabricated devices were exposed to the highest dose rate as 8.74 mGy s^{-1} for 150s, and then X-ray radiation was stopped for 300s. These steps were realized for other dose rates. After monitoring of the device responses to decreasing the dose rate, next step which, is increasing dose rates measurement were realized. It could be said that all three blend structured devices showed similar response characteristics as saw-tooth shaped for each X-ray dose rate in both regions. Afterwards to investigate repeatability in the X-ray responses, the same dose rate radiation 3.15 mGy s^{-1} were exposed onto P3HT:PCBM (1:1) dose rate for five times and presented in Fig. 7 (b). It can be obtained from Fig. 7 (b) repeatability of the device is very high for every X-ray on and off conditions.

The current densities of the three devices exposed to 3.15 mGy s^{-1} were plotted in Fig. 8 (a). The current density of the P3HT:PCBM (1:1) is higher than P3HT:PCBM(1:0.5) and P3HT:PCBM(1:2). According to Fig. 8(a), it could be said that current density was enhanced with loading ratio. But the current density of the P3HT:PCBM (1:1) is better than the device with the highest loading rate (as P3HT:PCBM(1:2)). Created excitons can be dissociated very easily with low bias voltage (in other words, in the presence of an electric field) due to the donor-acceptor interface. Mostly, diffusion length of the excitons in organic polymers is very short so the diffusion length of the exciton generated by optical excitation is critical at this point. PCBM has a key role for separation of excitons as free charges in the polymer bulk and can be enhanced with increasing PCBM ratio versus to major organic polymer materials. With the increase in the PCBM ratio in the base polymer (P3HT), the yield of exciton dissociation in the P3HT:PCBM bulk structure formed as a result of optical excitation can be enhanced. However, in a high loading ratio PCBM into the P3HT, the mobility of the free charge may be reduced and this causes to a decline in device performance. The X-ray sensitivity (S) of the devices is calculated with equation (1) as below.

$$S = \frac{\int \left[I_{X-ray\ On}(t) - I_{X-ray\ Off} \right] dt}{D \times V} \quad (1)$$

where, $I_{X\text{-ray on}}$ and $I_{X\text{-ray off}}$ are the current under X-ray exposure and in the dark conditions, respectively. D is the dose rate and V is the volume of the active area. Sensitivity values of the P3HT:PCBM based devices is given in Fig. 8 (b). Maximum S value was achieved with P3HT:PCBM (1:1) ratio as 655.47 µC mGy^{-1} cm^{-3}. Thirimanne et al. investigated

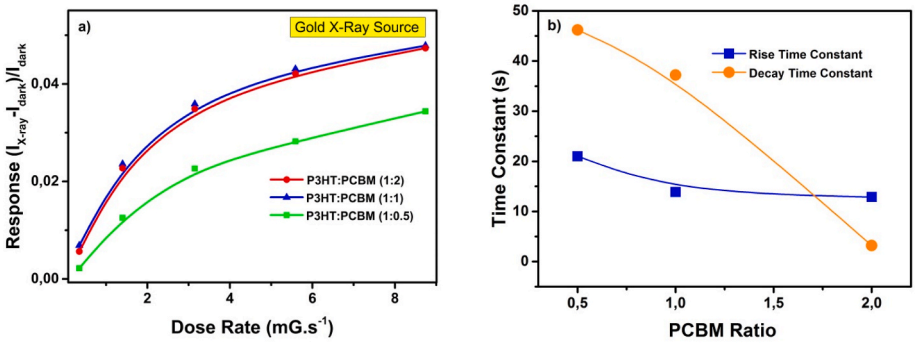

Fig. 9. Response versus Dose rate graphs for different PCBM loading ratio (a) and Rise and decay time constants for devices with increasing PCBM loadings under 10 V bias (b).

Table 1
Calculated absorption and attenuation coefficients of the common electrode materials and the Graphite.

Material	Atomic Number	Coherent Scattering ($x10^{-2}$ cm^2/g)	Incoherent Scattering ($x10^{-2}$ cm^2/g)	Photoelectric Absorption ($x10^{-2}$ cm^2/g)	Total Attenuation Without Coherent Scattering (x10-1 cm2/g)
Aluminum (Al)	13	10.9	14.6	87.2	10.2
Gold (Au)	79	132.3	8.4	2611	262.0
Nickel (Ni)	28	33.0	12.9	988.3	100.1
Palladyum (Pd)	46	62.8	10.5	3391	340.2
Graphite(C)	6	3.37	1.7	5.7	2.23

P3HT:PCBM based organic-inorganic hybrid X ray detectors with diode structure. To enhance device performance and sensitivity, Bi_2O_3 nanoparticles with different dimension were added into the active layer. So they achieved sensitivity as 1712 μC mGy^{-1} cm^{-3} for 80 nm Bi_2O_3 nanoparticles [16]. Valitova et al. investigated P3HT active layer based devices with diode structure as X ray detectors and achieved 22.9 nC/Gy sensitivity value [20]. According to literature survey, P3HT:PCBM based X ray detectors have been used as diode structure. In contrast, in this work we used resistive type device structure and acquired comparable sensitivity values.

Responses of the P3HT based devices loaded with various concentration of the PCBM depend on the X-ray dose rates were presented in Fig. 9 (a). The responses of the all fabricated devices increased with the increasing of the dose rates. According to Fig. 9 (a), all fabricated devices show exponential responses while increasing X-ray dose rates. This phenomenon could be attributed to the X-ray mass attenuation coefficient [33]. When X-ray has been exposed to any material (including air) photons interact with atoms or molecules by scattering or absorbing processes. If the photon energy is increased, the probability of interaction in the matter decreases [34]. Li. et al. investigated lead free polymer composites depended on the polymer contents and thickness of the materials. X-ray attenuation coefficient of the polymer based materials increased with the composite content and film thickness [35]. As a result, slope of the response to dose rate decreases with the increasing of the X-ray energy. The rise and decay times due to the loaded PCBM ratio were plotted in Fig. 9 (b). The rise times of the fabricated devices approximately decrease very rapidly. On the other hand, the decay time smoothest out more slowly. Thus, it could be said that recovering of the loading ratio has less importance than response time.

Besides loading of PCBM in P3HT at different rates, for X-ray detection, another original aspect of this work is the use of soluble Graphite electrode. The top electrode absorbs some of the incoming X-ray towards the device as a disadvantage. Especially in large-area applications, the use of less X-ray absorbing electrodes will reduce the negative effects of this disadvantage. Table 1 shows the comparison of absorption and attenuation coefficients of the common electrode materials used in device applications and the Graphite. Calculations are based on the NIST data for X-ray interaction cross sections and material densities. Considering these issues, graphite was chosen as the electrode material in this study.

The dominant physical phenomenon that causes the X-ray to be attenuated by the top electrode and prevents it from reaching the active layer of the detector is the photo-electric effect. Also, even if the coherent scattering values are given in the table to allow comparison, incoherent scattering causes the attenuation relatively. Therefore, incoherent scattering effects were not considered when calculating the total attenuation coefficients. When the calculated absorption and attenuation values are considered, the positive effect of the use of graphite electrodes is clear.

4. Conclusions

In this paper P3HT:PCBM active layer based X-ray detectors were fabricated and effect of PCBM ratio was investigated. All devices were constructed of the bulk resistive type with ohmic contacts. Spray coated graphite electrode was used as the top ohmic contact for all devices. P3HT:PCBM ratio was changed as (1:0), (1:0.5), (1:1), (1:2) and investigate PCBM concentrations how effect X-ray detection parameters with different X-ray dose rates under 10 V bias. Photocurrent of the pure P3HT (1:0) based device increased under X-ray exposure but never reached to a steady state level. However, when PCBM loaded into the P3HT photocurrent reached steady state current for all PCBM concentrations. X-ray dose rates were changed form 0.35 mGy s^{-1} to 8.74 mGy s^{-1} for all devices. To investigate potential usage of the produce organic polymer based materials as a direct radiation detectors, photocurrent measurement were realized with in first decreasing and then increasing X-ray radiation dose rates. The photocurrent versus time graph characteristic for PCBM loaded P3HT based devices were saw-tooth shaped depend on positive effects of PCBM ration on the diffusion length and mobility of the blended organic materials. Furthermore, PCBM loaded P3HT devices presented almost same photo-responses and this could be evaluated as repeatability parameters of fabricated detectors device and also could be said that has very good potential for usage in direct radiation detectors. Considering the calculated X-ray absorption and attenuation coefficients, the superiority of the use of graphite electrodes has been demonstrated.

Declaration of competing interest

The authors declare the following financial interests/personal relationships which may be considered as potential competing interests: Arif Kosemen reports article publishing charges, equipment, drugs, or supplies, and travel were provided by Turkish Energy Nuclear and Mining Research Institute.

Data availability

No data was used for the research described in the article.

Acknowledgment

This study was supported by Turkish Energy, Nuclear and Mineral Research Agency. Project number:. 2020 TENMAK(CERN)A5.H1.F5-27 and Scientific Research Projects Coordination Unit of Istanbul University-Cerrahpasa. Project number:. FBA-2021-35885.s

References

[1] J.S. Iwanczyk (Ed.), Radiation Detectors for Medical Imaging, CRC Press, 2015, 45.
[2] G. Harding, B. Schreiber, Radiat. Phys. Chem. 56 (1999) 229–245.
[3] C. Favuzzi, N. Giglietto, M.N. Mazziotta, P. Spinelliet, Transition radiation detectors for particle physics and astrophysics, Riv. Nuovo Cim. 24 (2001) 1–172.
[4] K. Iniewski, Electronics for Radiation Detection, CRC Press, 2018.
[5] A.J.J. Bos, High sensitivity thermoluminescence dosimetry, Nucl. Instrum. Methods Phys. Res. B 184 (2001) 28, 3.
[6] A. Intaniwet, C.A. Mills, P.J. Sellin, M. Shkunov, J.L. Keddie, Achieving a stable time response in polymeric radiation sensors under charge injection by X-rays, ACS Appl. Mater. Interfaces 2 (6) (2010) 1692–1699.
[7] L. Basiricò, A. Ciavatti, T. Cramer, Direct X-ray photoconversion in flexible organic thin film devices operated below 1 V, Nat. Commun. 7 (2016), 13063.

[8] A. Owens, A. Peacock, Compound semiconductor radiation detectors, Nucl. Instrum. Methods Phys. Res. Sect. Accel. Spectrometers Detect. Assoc. Equip. 531 (2004) 18–37.
[9] P. Zygmanski, C. Abkai, Z. Han, Y. Shulevich, D. Menichelli, Low-cost flexible thin-film detector for medical dosimetry applications, J. Appl. Clin. Med. Phys. 15 (2014) 4454.
[10] K. Wang, F. Chen, G. Belev, S. Kasap, K.S. Karim, Lateral metal-semiconductor-metal photodetectors based on amorphous selenium, Appl. Phys. Lett. 95 (2009), 013505.
[11] M. Bruzzi, C. De Angelis, M. Scaringella, C. Talamonti, D. Viscomi, M. Bucciolini, Zero-bias operation of polycrystalline chemically vapour deposited diamond films for Intensity Modulated Radiation Therapy, Diam. Relat. Mater. 20 (2011) 84–92.
[12] S. Lee, J. Hong, J.H. Koo, S. Lee, K. Lee, S. Im, T. Lee, Single-crystalline silicon based heterojunction photodiode arrays on flexible plastic substrates, IEEE Trans. Electron. Dev. 58 (2011) 3329–3334.
[13] N. Tessler, N.T. Harrison, R.H. Friend, Adv. Mater. 10 (1998) 64–68.
[14] A. Kosemen, High-performance organic field-effect transistors fabricated with high-k composite polymer gel dielectrics, J. Electron. Mater. 48 (2019) 12.
[15] K.M. Coakley, M.D. Mc Gehee, Chem. Mater. 16 (2004) 4533.
[16] H.M. Thirimanne, K.D.G.I. Jayawardena, A.J. Parnell, R.M.I. Bandara, A. Karalasingam, S. Pani, J.E. Huerdler, D.G. Lidzey, S.F. Tedde, A. Nisbet, C. A. Mills, S.R.P. Silva, High sensitivity organic inorganic hybrid X-ray detectors with direct transduction and broadband response, Nat. Commun. 9 (2018) 2926.
[17] L. Basiricò, A. Ciavatti, B. Fraboni, Solution-grown organic and perovskite X-ray detectors: a new paradigm for the direct detection of ionizing radiation, Adv. Mater. Technol. 6 (2021), 2000475.
[18] Y.L. Loo, I. McCulloch, Progress and challenges in commercialization of organic electronics, MRS Bull. 33 (2008) 653.
[19] F.C. Krebs, Roll-to-roll fabrication of monolithic large-area polymer solar cells free from indium-tin-oxide, Sol. Energy Mater. Sol. Cell. 93 (2009) 394.
[20] I. Valitova, A. Hupman, I.G. Hill, A. Syme, Poly(3-hexylthiophene-2,5-diyl) based diodes for ionizing radiation dosimetry applications, Org. Electron. 88 (2021), 105981.
[21] M.P.A. Nanayakkara, L. Matjačić, S. Wood, F. Richheimer, F.A. Castro, S. Jenatsch, S. Züfle, R. Kilbride, A.J. Parnell, M.G. Masteghin, H.M. Thirimanne, A. Nisbet, K. D.G. Imalka Jayawardena, S. Ravi P. Silva, Ultra-low dark current organic–inorganic hybrid X-ray detectors, Adv. Funct. Mater. 31 (2021), 2008482.
[22] F.A. Boroumand, M. Zhu, A.B. Dalton, J.L. Keddie, P.J. Sellin, J.J. Gutierrez, Direct x-ray detection with conjugated polymer devices, Appl. Phys. Lett. 91 (2007), 033509.
[23] A. Intaniwet, C.A. Mills, M. Shkunov, H. Thiem, J.L. Keddie, P.J.J. Sellin, Characterization of thick film poly(triarylamine) semiconductor diodes for direct x-ray detection, Appl. Phys. 106 (2009), 064513.
[24] A. Intaniwet, High charge-carrier mobilities in blends of poly(triarylamine) and TIPS-pentacene leading to better performing X-ray sensors, Org. Electron. 12 (11) (2011) 1903–1908.
[25] H. Han, S. Lee, J. Seo, C. Mahata, S. Hwan Cho, A.-R. Han, K.-S. Hong, J.-H. Park, M.-J. Soh, C. Park, T. Lee, Enhancement of X-ray detection by single-walled carbon nanotube enriched flexible polymer composite, Nanoscale Res. Lett. 9 (2014) 610.
[26] M.J. Griffith, S. Cottam, J. Stamenkovic, J.A. Posar, M. Petasecca, Printable organic semiconductors for radiation detection: from fundamentals to fabrication and functionality, Front. Physiol. (2020) 8.
[27] A. Ciavatti, L. Basiricò, I. Fratelli, S. Lai, P. Cosseddu, A. Bonfiglio, J.E. Anthony, B. Fraboni, Boosting direct X-ray detection in organic thin films by small molecules tailoring, Adv. Funct. Mater. 29 (2019), 1806119.
[28] M.A. Hupman, I. Valitova, I. Ghill, A. Syme, Method for the differentiation of radiation-induced photocurrent from total measured current in P3HT/PCBM BHJ photodiodes, MethodsX 7 (2020), 101125.
[29] I. Valitova, A. Hupman, I.G. Hill, A. Syme, Poly(3-hexylthiophene-2,5-diyl) based diodes for ionizing radiation dosimetry applications, Org. Electron. 88 (2021), 105981.
[30] F.V. Molefe, Spectroscopic investigation of charge and energy transfer in P3HT/GO nanocomposite for solar cell applications, Adv. Mater. Lett. 8 (3) (2017) 246–250.
[31] J.U. Lee, J.W. Jung, T. Emrick, T.P. Russell, W.H. Jo, Synthesis of C60-end capped P3HT and its application for high performance of P3HT/PCBM bulk heterojunction solar cells, J. Mater. Chem. 20 (2010) 3287–3294.
[32] G. Pace, A. Grimoldi, D. Natali, M. Sampietro, J.E. Coughlin, G.C. Bazan, M. Caironi, Development of organic semiconductor photodetectors: from mechanism to applications, Adv. Mater. 26 (2014) 6773.
[33] N. Nagaraja, K.N. Sridhar, H.C. Manjunatha, Y.S. Vidya, L. Seenappa, P. S. Damodara Gupta, H.B. Ramalingam, Measurement of mass attenuation coefficient and its derivable in polymers, Prog. Nucl. Energy 144 (2022), 104044.
[34] L. Xiang, X. Huang, Y. Wang, Z. Xin, G. Chai, Y. Xu, K. Wang, J. Chen, C. Liu, X. Wang, S. Zhang, H. Zhou, X-ray Sensitive hybrid organic photodetectors with embedded CsPbBr3 perovskite quantum dots, Org. Electron. 98 (2021), 106306.
[35] Z. Li, W. Zhou, X. Zhang, Y. Gao, S. Guo, High-efficiency, flexibility and lead-free X-ray shielding multilayered polymer composites: layered structure design and shielding mechanism, Sci. Rep. 11 (2021) 4384.